

1 **Genetic variation of heat tolerance in a model**
2 **ectotherm: an approach using thermal death time curves**

3
4 Félix P. Leiva^{1,2,*}, Mauro Santos^{3,4}, Edwin J. Niklitschek^{5,6}, Enrico L. Rezende⁷ and
5 Wilco C.E.P. Verberk²

6
7 ¹Alfred Wegener Institute, Helmholtz Centre for Polar and Marine Research, 27570 Bremerhaven,
8 Germany

9 ²Department of Ecology, Radboud Institute for Biological and Environmental Sciences, Radboud
10 University Nijmegen, 6500 GL Nijmegen, The Netherlands

11 ³Departament de Genètica i de Microbiologia, Grup de Genòmica, Bioinformàtica i Biologia Evolutiva
12 (GBBE), Universitat Autònoma de Barcelona, Bellaterra, Barcelona 08193, Spain

13 ⁴Institute of Evolution, Centre for Ecological Research, Konkoly-Thege Miklós út 29-33, H-1121,
14 Budapest, Hungary

15 ⁵Centro i-mar, Universidad de Los Lagos, Km 6, Camino a Chiquihue, Casilla 557, Puerto Montt
16 5480000, Chile

17 ⁶Universidad Austral de Chile, Programa de Investigación Pesquera UACH-ULAGOS, Los Pinos S/N,
18 Puerto Montt 5480000, Chile

19 ⁷Departamento de Ecología, Center of Applied Ecology and Sustainability (CAPES), Facultad de
20 Ciencias Biológicas, Pontificia Universidad Católica de Chile, Santiago 6513677, Chile

21 *Corresponding author e-mail: felixpleiva@gmail.com

22
23 Word counts: 3,271 out of 3,500 words

24

25 **Abstract**

26 The assessment of thermal tolerance holds significant importance in predicting the
27 physiological responses of ectotherms, particularly in elucidating their capacity for
28 evolutionary adaptation in the context of global warming. Current approaches to assessing
29 thermal tolerance have limitations that can lead to misleading results, especially with regard
30 to the heritability of thermal limits. In this study, we examined twenty isogenic lines of
31 *Drosophila melanogaster* from the DGRP panel to characterize their thermal death time (TDT)
32 curves, which account for the duration and intensity of heat stress. Furthermore, we examined
33 the extent of genetic variation in the two parameters that characterize TDT curves, namely
34 CTmax and thermal sensitivity z . Our analysis revealed evidence of genetic (co)variation for
35 both parameters. Results from simulations of the evolutionary consequences of selection on
36 CTmax and z suggest that directional selection to increase CTmax will also increase z as a
37 correlated response. However, directional selection to increase z may have the opposite
38 effect. We conclude that the evolution of thermosensitive or thermotolerant strategies is better
39 achieved by directional selection to decrease or increase CTmax, which may aid in mitigating
40 the effects of global warming on ectotherms.

41

42 **Keywords:** global warming, heritability, isogenic lines, thermal death time curves

43

44 1. Introduction

45 There is substantial evidence pointing to an unprecedented rise in the temperature of our
46 planet. According to climate models, if the present warming trends persist, the surface
47 temperature of the Earth's surface will surpass the average at the end of the 19th century by
48 1.5°C [1]. It is not surprising that this rise will have repercussions on the biota present on our
49 planet, particularly for animals such as ectotherms, whose physiological processes are closely
50 linked to ambient temperature [2,3]. Climate change is already having an impact at the
51 demographic level. Many species are shifting their ranges, often towards cooler regions [4],
52 while others are threatened with extinction [5]. There is ample evidence that some species
53 might be able to adapt to rising temperatures through the evolution of heritable stress-tolerant
54 phenotypes [6]. Some lineages are already able to withstand high temperatures [7], while
55 others show phenotypic plasticity [8], and some species may evolve in response to warming
56 [6,9]. Assessing the adaptive capacity and heritability of heat tolerance is challenging, as
57 inaccuracies in models can lead to either under- or overestimation of vulnerability to climate
58 change [10,11].

59 The current debate about the evolutionary potential of heat tolerance in ectotherms
60 can be summarized in two main points. First, there is the notion that ectotherms possess
61 limited plasticity for heat tolerance, suggesting that heat tolerance is both evolutionary and
62 physiologically fixed. Natural selection appears to affect physiological responses to lower
63 temperatures more than to higher temperatures [12]. Interspecific studies - i.e., among species
64 - have failed to detect genetic variability in heat tolerance, variation between species and
65 populations, and a lack of latitudinal diversity [13,14]. Likewise, selection and heritability
66 experiments on single species suggest limited increases in upper thermal limits. Second, a
67 complicating factor in understanding the genetic basis of upper thermal limits is that these are
68 to some extent affected by methodological issues [for a review, see 12]. Heat tolerance is
69 often estimated using ramping assays to assess upper critical thermal limits (CT_{max}), which
70 are the maximum ambient temperatures that an ectotherm can tolerate under a given
71 experimental condition before succumbing to heat [15]. However, this approach is difficult to
72 replicate at the individual level, especially when mortality is the measured endpoint [11]. The
73 conclusion of these studies is clear and suggests a limited evolutionary potential for
74 ectotherms to increase their ability to tolerate high temperatures. Despite the possibility of
75 methodological issues underestimating the actual evolutionary potential to withstand
76 increasing temperatures [10], it is imperative to acknowledge that CT_{max} is merely a
77 component of the more intricate trait "thermal tolerance" [16].

78 An increasing number of studies have employed thermal death time (TDT) curves to
79 measure heat tolerance [17–22]. However, the extent to which TDT curves reflect evolutionary
80 changes within a species remains unclear. TDT curves imply that an individual's survival
81 probability is influenced by both temperature and exposure time [23], and may provide a more
82 nuanced view of the two reasons mentioned above for the ongoing debate. In this context, we
83 take advantage of recent research using the *Drosophila* Genetic Reference Panel (DGRP)
84 [16,24] to investigate the genetic variation of heat tolerance in *Drosophila melanogaster* using
85 TDT curves. The wild-type DGRP lines of this panel are derived from a single natural
86 population and have been inbred to homozygosity, providing extensive information on genetic
87 variation at multiple levels [25] and offering unique opportunities to quantify the genetic basis
88 of physiological traits such as heat tolerance.

89 2. Material and methods

90 (a) Experimental flies and rearing conditions

91 Twenty inbred, isogenic wild-type *Drosophila melanogaster* (Meigen 1830) lines from the
92 *Drosophila* Genetic Reference Panel (DGRP) were used as the study model. These lines were
93 previously employed in a study with a different objective [19], and we assume that this subset
94 represents an approximately random collection with respect to the focus of interest described
95 here.

96 All twenty selected lines were obtained from the Bloomington *Drosophila* Stock Center
97 in March 2018. They were maintained in quarantine on standard cornmeal-agar-yeast media
98 at room temperature (approximately 22°C) for four generations until May 2018. The rearing
99 conditions were identical to those detailed in Leiva et al. [19].

100 (b) Thermal death time (TDT) curves

101 We measured the heat tolerance of individual female and male flies using a similar
102 experimental protocol as outlined in Verspagen et al. [22]. This involved using a heating
103 circulating bath and a wireless thermometer to measure temperature consistently throughout
104 each trial. Individual virgin flies were placed in sealed 4-mL glass vials, arranged on a
105 Plexiglas™ rack, and submerged in a 9.5-L glass aquarium filled with water set to a constant
106 temperature of 36, 37, 38, or 39°C. During each trial, a Nikon D5300 with the time-lapse
107 feature captured images at 10-second intervals. Subsequently, the compiled images were
108 transformed into reversed videos using the open-source software Blender. Before initiating
109 the thermal tolerance experiments, the flies were allowed approximately 30 minutes in the
110 vials at room temperature for recovery following light CO₂ anaesthesia. This recovery period
111 proved effective, as the flies exhibited active flying or walking inside the vial.

112 A total of 1,686 flies underwent survival time measurements, and the parameters of
113 the thermal death time (TDT) curves (CT_{max} and *z*) were calculated for each DGRP line and
114 sex. The calculation utilized the equation outlined in Rezende et al. [23]:

$$115 \log_{10} t = \frac{CT_{\max} - T}{z} \quad (1)$$

116 where *t* represents the survival time in minutes, CT_{max} is the temperature (°C) where the
117 survival time is log₁₀ *t* = 0 after 1 min of exposure to assay temperature, *T* is the assay
118 temperature (°C), and the thermal sensitivity *z* is the temperature change (°C) required for a
119 ten-fold difference in survival time. We maintained control over assay temperature (*T*) and
120 measured time (*t*) as the dependent variable. The estimation of CT_{max} and *z* for each DGRP
121 line and sex involved regression analysis of log₁₀-transformed survival times against the four
122 temperature treatments.

123 (c) Estimation of variance components and broad-sense heritability of CT_{max} and *z*

124 For each DGRP genotype, we first assessed the effect of stressful temperatures (covariate)
125 on survival time (in log₁₀ min) by using for each sex the following general mixed ANCOVA
126 model that allows separating slopes and intercepts:

127 $Survival\ time = \beta_0 + \beta_1 \cdot stress\ T^a + \mu_0 Z + \mu_1 Z \cdot stress\ T^a + \varepsilon$ (2)

128 where

129 β_0 and β_1 : intercept and slope of the fixed effect of stress temperature $stress\ T^a$,

130 $\mu_0 \sim N(0, G_{1,1})$: vector of random coefficients representing the effect of each genotype on β_0 ,

131 $\mu_1 \sim N(0, G_{2,2})$: vector of random coefficients representing the effect of each genotype on β_1 ,

132 Z : Design matrix (array of dummy variables) representing the genotypes,

133 G : variance-covariance matrix for the random effects,

134 ε : vector of random errors

135 We fitted linear mixed-effects models [26] and obtained various estimates of the
 136 variance components $\hat{\sigma}_{\hat{\beta}_{0i}}^2$ ($i = 1, \dots, 20$), $\hat{\sigma}_{\hat{\beta}_{1i}}^2$ and $\hat{\sigma}_{\varepsilon}^2$ (caret denotes "estimate") that refer,
 137 respectively, to the variation in the intercepts and slopes of the TDT curves for the DGRP
 138 genotypes, and the residual variation. Model coefficients and variance components were then
 139 used to estimate $CT_{max} = \beta_1/\beta_0$ and $z = -1/\beta_1$, whose Taylor expanded variances [27, p. 240],
 140 became,

141
$$\text{Var}(CT_{max_i}) = \text{Var}\left(\frac{-\hat{\beta}_{0i}}{\hat{\beta}_{1i}}\right) \approx \frac{(\mu_{-\hat{\beta}_{0i}})^2}{(\mu_{\hat{\beta}_{1i}})^2} \left[\frac{\hat{\sigma}_{-\hat{\beta}_{0i}}^2}{(\mu_{-\hat{\beta}_{0i}})^2} + \frac{\hat{\sigma}_{\hat{\beta}_{1i}}^2}{(\mu_{\hat{\beta}_{1i}})^2} - 2 \frac{\text{Cov}(-\hat{\beta}_{0i}, \hat{\beta}_{1i})}{\mu_{-\hat{\beta}_{0i}} \mu_{\hat{\beta}_{1i}}} \right]$$

142 (3)

143
$$\text{Var}(z_i) \approx \frac{\hat{\sigma}_{\hat{\beta}_{1i}}^2}{(\mu_{\hat{\beta}_{1i}})^4}$$

144 We then estimated broad-sense heritability as:

146
$$H_{CT_{max}}^2 = \frac{\text{Var}(CT_{max_i})}{\text{Var}(CT_{max_i}) + \text{Var}(z_i) + \frac{\hat{\sigma}_{\varepsilon}^2}{n_0}}$$

145 (4)

148
$$H_z^2 = \frac{\text{Var}(\hat{z}_i)}{\text{Var}(CT_{max_i}) + \text{Var}(z_i) + \frac{\hat{\sigma}_{\varepsilon}^2}{n_0}}$$

147

149 where

151
$$n_0 = \frac{1}{a-1} \left(\sum_{i=1}^a n_i - \frac{\sum_{i=1}^a n_i^2}{\sum_{i=1}^a n_i} \right)$$

150 (5)

152 is the appropriate mean value of the number of flies from each sex and DGRP line used at
 153 each stressful temperature to estimate the TDT curves [28, p. 212] The reason we divided the
 154 residual variance by n_0 is because we are using line means [29]. In our case $n_0 = 10.2480$
 155 for females and $n_0 = 10.8055$ for males.

156 Delete-one-DRGP genotype at a time data resampling was also carried out to estimate
 157 the genetic components of variance and their standard errors [30]. A total of 20 pseudovalues
 158 for each sex were obtained by dropping, in turn, each DGRP line and calculating:

160
$$\phi_i = N\hat{\theta}_N - (N-1)\hat{\theta}_{N-1,i}$$

159 (6)

161 where ϕ_i is the i th pseudovalue, $\hat{\theta}_N$ is the corresponding variance estimate using all $N = 20$
 162 DGRP genotypes, and $\hat{\theta}_{N-1,i}$ is that estimate by dropping the i th DGRP genotype alone. The
 163 jackknife estimate is the average of ϕ_i , and its standard error is given by

165
$$SE = \sqrt{\frac{\sum_{i=1}^{i=N} (\phi_i - \bar{\phi})^2}{N(N-1)}}$$

164 (7)

166 Approximate 95% jackknife confidence intervals were obtained as $\bar{\phi} \pm 2 SE$. Initially,
 167 the analyses for computing variance components and heritability were implemented by MS in
 168 MATLAB. To enhance reproducibility, FPL and EJM replicated the analyses and implemented
 169 them in R version 4.3.2 [31]. The data used in these analyses were based on a recently
 170 reported study [19,32].

171 (d) Hypothetical selection on the TDT curves

172 Appropriate estimates of the additive-genetic G and phenotypic P (co)variance matrices in an
 173 outbred *Drosophila* population are needed to explore the hypothetical evolutionary
 174 consequences of selection on CTmax and z from the multivariate breeder's equation $\Delta\mu =$
 175 $G\beta = GP^{-1}s$. Here, the term $\Delta\mu$ is the vector of changes in trait means, β is the vector of
 176 selection gradients, and s is the vector of selection differentials [33,34].

177
 178
 179 The estimates of genetic variance-covariance components and broad-sense
 180 heritability in the highly inbred DGRP lines yield only the relative contributions of CTmax and
 181 z to the total genetic variance in the TDT curves [see 29]. To our knowledge, there are no
 182 estimates of the narrow-sense heritability of TDT curves. Current evidence suggests that
 183 CTmax (estimated by different methodologies) is moderately heritable, and it seems
 184 reasonable to assume that its narrow-sense heritability is $h_{CTmax}^2 \approx 0.25$ [35–37]. Based on

185 this information and the relative contribution of CTmax and z to the total genetic variance of
186 TDT curves, we approached the hypothetical consequences of several selective scenarios on
187 the evolution of thermal tolerance (represented by these two parameters in the TDT curves)
188 in an outbred population. Note that this will be “what-if” scenarios and more accurate estimates
189 of G and P would be needed for a more satisfactory answer.

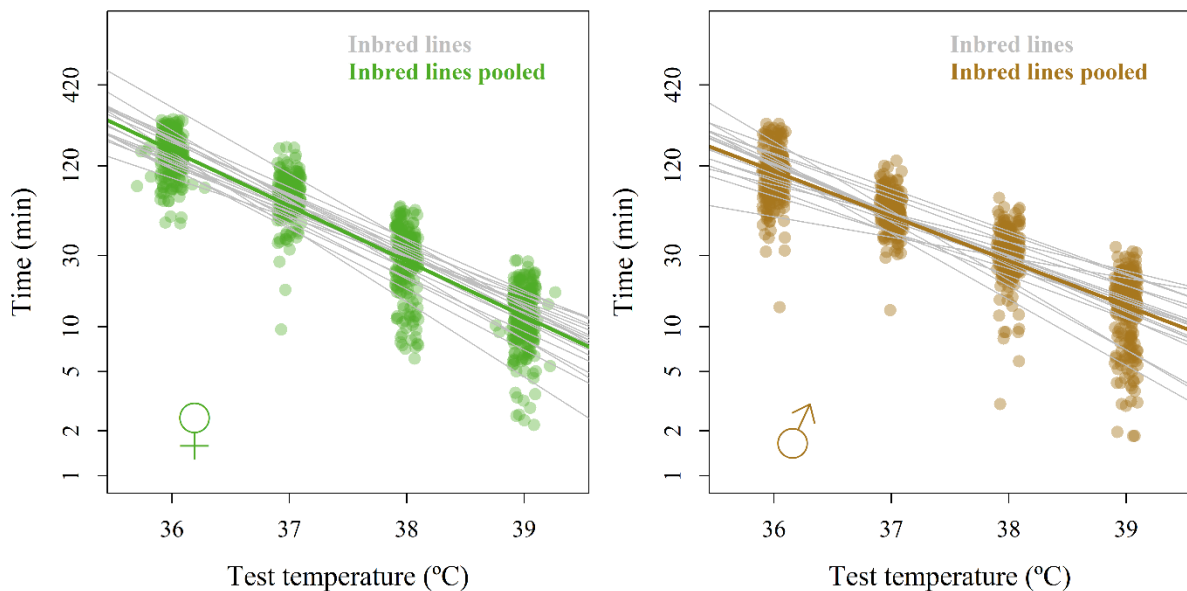
190 3. Results

191 (a) Determination of TDT curves and variance components

192
193 We observed substantial variation in thermal death time (TDT) curves across genetic lines for
194 both females and males (Figure 1). At 36°C, the average survival times (\pm SD) were 150 ± 47
195 minutes for females and 111 ± 41.6 minutes for males. These durations decreased
196 significantly at 39°C, with females surviving for 12.7 ± 5.13 minutes and males for 14.7 ± 5.6
197 minutes on average. Notably, this variation in thermal tolerance across genetic lines was
198 consistently observed for both sexes (Figure 1).

199
200 Table 1 provides estimates of the variance-covariance components and broad-sense
201 heritability using different methods for estimating parameters in the linear mixed-effects model.
202 These estimates were highly consistent across the various methods of estimation. As
203 indicated by the jackknife 95% confidence intervals, all variance components were
204 significantly different from zero. Furthermore, the genetic covariance between β_0 and β_1 was
205 negative. Broad-sense heritability was around 0.75 for CTmax and around 0.25 for z. In other
206 words, CTmax accounts for approximately 75% and z accounts for approximately 25% of the
207 total genetic variance in the TDT curves.

208



209
210 **Figure 1.** Thermal death time (y-axis in log₁₀-scale) curves for females (left) and males (top). Dots
211 represent the individual survival time for females (green, left plot) and males (brown, right plot).

212

213

214

215
216

Table 1. Estimates of variance-covariance components and broad-sense heritability using various methods for estimating parameters in the linear mixed-effects model.

Method	Component	Females				Males			
		Estimate	Jackknife	Lower 95% CI	Upper 95% CI	Estimate	Jackknife	Lower 95% CI	Upper 95% CI
ANOVA	$\hat{\sigma}_{\beta_{0i}}^2$	4.611517	4.611517	1.497235	7.725798	8.513706	8.513706	2.164972	14.862439
	$\hat{\sigma}_{\beta_{1i}}^2$	0.003349	0.003349	0.001044	0.005654	0.006193	0.006193	0.001611	0.010775
	$Cov(\hat{\beta}_0, \hat{\beta}_1)$	-0.124158	-0.124158	-0.208805	-0.039511	-0.229524	-0.229524	-0.400045	-0.059003
	σ_ε^2	0.025323	0.025350	0.017416	0.033283	0.022589	0.022626	0.016258	0.028993
	$\sigma_{C_{Tmax}}^2$	0.627648	0.636561	0.168601	1.104520	2.291032	2.295229	0.810871	3.779587
	σ_z^2	0.177251	0.178170	0.061913	0.294427	0.741910	0.733917	0.182960	1.284875
	$H_{C_{Tmax}}^2$	0.777398	0.785244	0.713835	0.856653	0.754862	0.753906	0.707689	0.800124
	H_z^2	0.219542	0.212210	0.142225	0.282195	0.244449	0.245497	0.198955	0.292039
ML	$\hat{\sigma}_{\beta_{0i}}^2$	3.632183	3.814144	0.871781	6.756507	7.511015	7.925969	1.961018	13.890921
	$\hat{\sigma}_{\beta_{1i}}^2$	0.002667	0.002805	0.000612	0.004998	0.005478	0.005781	0.001472	0.010091
	$Cov(\hat{\beta}_0, \hat{\beta}_1)$	-0.098333	-0.103146	-0.183387	-0.022905	-0.202835	-0.214073	-0.374373	-0.053773
	σ_ε^2	0.025342	0.025379	0.017435	0.033323	0.022591	0.022629	0.016262	0.028995
	$\sigma_{C_{Tmax}}^2$	0.544844	0.699675	0.213560	1.185790	1.984050	2.096104	0.709432	3.482775
	σ_z^2	0.142061	0.150940	0.039450	0.262430	0.657861	0.687462	0.171167	1.203756
	$H_{C_{Tmax}}^2$	0.790341	0.837934	0.747598	0.928270	0.750397	0.749330	0.698801	0.799859
	H_z^2	0.206072	0.160207	0.071933	0.248481	0.248813	0.250045	0.199158	0.300933
REML	$\hat{\sigma}_{\beta_{0i}}^2$	3.860733	3.812656	0.707172	6.918140	7.936582	7.926299	1.627602	14.224995
	$\hat{\sigma}_{\beta_{1i}}^2$	0.002833	0.002803	0.000489	0.005117	0.005787	0.005782	0.001232	0.010332
	$Cov(\hat{\beta}_0, \hat{\beta}_1)$	-0.104485	-0.103195	-0.187844	-0.018545	-0.214315	-0.214085	-0.383354	-0.044816
	σ_ε^2	0.025341	0.025378	0.017435	0.033321	0.022591	0.022629	0.016262	0.028995
	$\sigma_{C_{Tmax}}^2$	0.576073	0.642215	0.134858	1.149572	2.094327	2.096591	0.632687	3.560495
	σ_z^2	0.150863	0.150927	0.033324	0.268531	0.694961	0.687087	0.141802	1.232372
	$H_{C_{Tmax}}^2$	0.789781	0.817682	0.741656	0.893708	0.750284	0.749375	0.699061	0.799689
	H_z^2	0.206829	0.180052	0.106313	0.253791	0.248967	0.249991	0.199340	0.300642

217
218

219 **(b) Hypothetical selection on the TDT curves**

220

221 We can employ the raw phenotypic (co)variance matrix of the females from the DGRP lines
222 as a representative of the \mathbf{P} matrix in an outbred population, omitting any changes in
223 phenotypic variance caused by inbreeding for the sake of simplicity [38]. Assuming absence
224 of epistasis, the genetic variation in the DGRP lines for CTmax and z (REML estimates for
225 females in Table 1) has been rescaled so that $h_{CTmax}^2 \approx 0.25$ and $h_z^2 \approx 0.07$. Hence, we
226 presume the subsequent (co)variance genetic, environmental, and phenotypic matrices for
227 CTmax and z in the hypothetical outbred base population:

228

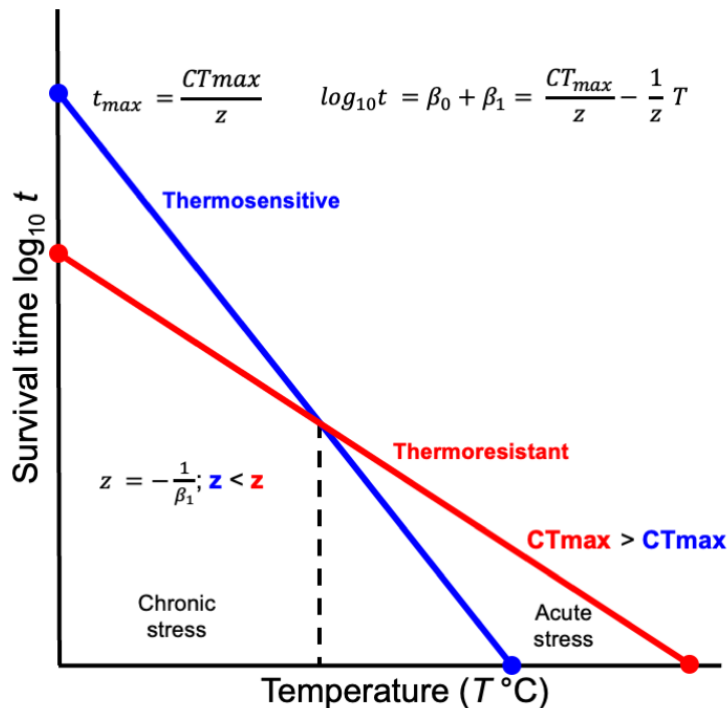
$$229 \quad G = \begin{bmatrix} 0.1489 & 0.0423 \\ 0.0423 & 0.0133 \end{bmatrix}; \quad E = \begin{bmatrix} 0.4466 & 0.2618 \\ 0.2618 & 0.1691 \end{bmatrix}; \quad P = \begin{bmatrix} 0.5955 & 0.3041 \\ 0.3041 & 0.1823 \end{bmatrix}$$

230

231 The vector of phenotypic means in this base population is $\bar{\mu} = [41.9924 \quad 2.7592]^T$
232 (T stands for transpose), where the first value is for CTmax and the second for z (female
233 means from the DGRP lines). We assume that these values are representative of the outbred
234 population, which is strictly true if allelic effects are additive [39].

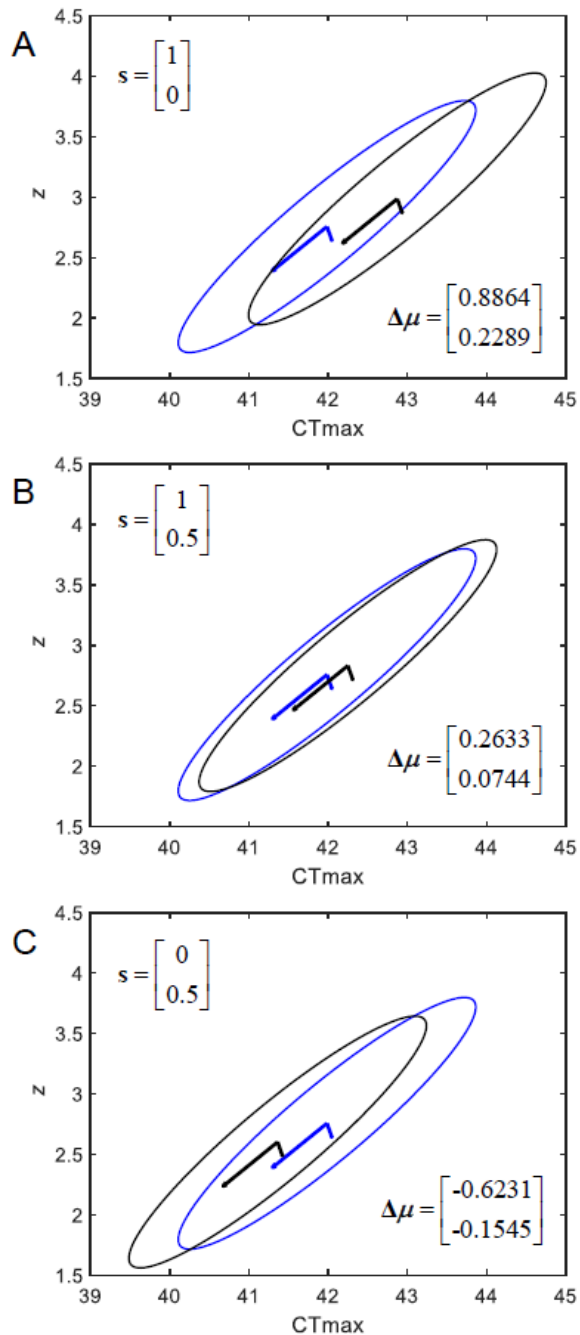
235

236 We simulated three scenarios for increasing thermoresistance (Figure 2): directional
237 selection for CTmax ($s = [1 \quad 0]^T$), directional selection for both CTmax and z
238 ($s = [1 \quad 0.5]^T$), and directional selection for z ($s = [0 \quad 0.5]^T$). These selection differentials
239 correspond to intensities of selection $i_{CTmax} = 1.3$ and $i_z = 1.2$. The hypothetical selection
240 regimes used to illustrate the effects of selection are much stronger than we would expect in
241 nature because directional selection tends to be weak and rarely shifts mean by more than
242 half of a phenotypic standard deviation [40,41]. However, under extreme climatic events, such
243 as heat waves, which are considered to be major triggers of evolution [42], these intensities
244 of selection may not be unrealistic [43].



245
 246 **Figure 2.** The thermal death time (TDT) curve linearly describes the relationship between test
 247 temperature (T) and survival time (t , \log_{10} scale) under heat stress conditions in *D. melanogaster*.
 248 Thermal sensitivity (z) is the reciprocal of the slope (β_1), representing the increase in temperature
 249 required to reduce survival time by one order of magnitude (10-fold). CT_{max} is the intersection at \log_{10}
 250 = 0, corresponding to the knockdown or death temperature after 1 minute of exposure. The blue line
 251 represents a thermosensitive genotype, which exhibits improved tolerance to acute, intense heat stress
 252 but reduced tolerance to chronic, less intense heat. Conversely, the red line depicts a thermoresistant
 253 genotype, exhibiting better tolerance to chronic stress but lower tolerance to acute stress.

254
 255 The simulated scenarios are shown in Figure 3. It is striking that a directional selection
 256 gradient always has a different sign than its selection differential, and the evolutionary
 257 response can be against the selection differential (Figure 3C). The inference from these
 258 hypothetical selection regimes is that directional selection to increase thermal sensitivity z
 259 seems to hinder evolutionary responses to increasing CT_{max} . In other words, directional
 260 selection to increase CT_{max} also increases z as a correlated response (Figure 3A) and, as
 261 expected, drives the population towards a more thermoresistant state (Figure 2). However,
 262 directional selection to increase z results in a decrease of CT_{max} as a correlated response,
 263 which, in turn, also decreases z , and seemingly paradoxically drives the population towards
 264 increasing thermosensitivity (Figure 2).



265
 266
 267
 268
 269
 270
 271
 272
 273
 274
 275
 276

Figure 3. Hypothetical strong directional selection for increased thermoresistance. In blue the 95% confidence ellipses of a simulated population of $N = 10,000$ flies from a bivariate normal distribution whose phenotypes for CTmax and z are the sum of genetic effects with mean $\bar{\mu} = [41.9924 \ 2.7592]^T$ and additive-genetic (co)variance G , plus environmental effects with mean 0 and (co)variance E (see text). The arrows centred on the bivariate means represent the directions in which the data vary the most (i.e., the eigenvectors of the covariance matrix of the data). In black are the 95% confidence ellipses after an evolutionary shift in the means (we ignore changes in variance and covariance). Panel A plots directional selection for increasing CTmax; the vector of selection gradients is $\beta = [11.3294 \ -18.8959]^T$. Panel B plots directional selection for increasing both CTmax and z , where $\beta = [1.8814 \ -0.3958]^T$. Panel C plots directional selection for increasing z , where $\beta = [-9.4480 \ 18.5002]^T$.

277 4. Discussion

278 Heat tolerance has traditionally been examined from a physiological perspective, with a focus
279 on the mechanisms that cause animals to succumb to heat stress, such as oxygen limitation
280 or excessive water loss [see 44 for a review]. In this study, we present a novel viewpoint by
281 examining the genetic components of heat tolerance through the lens of thermal death time
282 (TDT) curves. This allows partitioning the relative contribution of CT_{max} and *z* to the more
283 complex trait “thermotolerance” (Figure 2). Our approach has relied on inbred *Drosophila*
284 *melanogaster* lines from the DGRP panel, and it would be highly desirable to extend these
285 analyses to outbred populations.

286
287 The limited number of previous studies that have assessed the thermal tolerance of
288 DGRP lines focused primarily on measuring critical thermal limits [45,46]. These, along with
289 other studies [12,47], suggest that heat tolerance is somewhat evolutionary constrained, an
290 idea often invoked to explain the absence of strong latitudinal clines in heat tolerance [13].
291 Typically, assessments of organisms’ vulnerability to global warming usually compare
292 experimentally derived thermal limits using ramping trials, in which animals are exposed to
293 increasingly higher temperatures [15,48]. During these trials, the intensity and duration of
294 stress increase concurrently. As a result, animals often succumb to heat stress in rapid
295 succession, leading to small variances and small standard deviations in the measurements,
296 making CT_{max} an attractive endpoint to use in treatment comparisons. However, CT_{max} is a
297 single point, whereas the trait of interest, namely the ability of an organism to deal with heat
298 stress, is a linear function describing how stress intensity and stress duration impact survival
299 [23]. Thus, ramping trials approach overlooks the cumulative nature of heat injury and the
300 time-dependent effects of thermal tolerance [49–51], potentially underestimating organisms’
301 vulnerability to global warming [52]. We contend that utilizing TDT curves to evaluate both
302 CT_{max} and *z* parameters, as well as their underlying genetic basis, would provide more
303 accurate predictions. Here, we have developed a methodological approach to estimate the
304 variance components and heritability of the relevant parameters in the TDT curves.

305 The hypothetical selection scenarios allow us to understand how thermosensitive and
306 thermotolerant strategies (Figure 2) can evolve. These scenarios suggest that thermosensitive
307 or thermotolerant strategies are better achieved by directional selection to decrease or
308 increase CT_{max}. This conclusion holds in more realistic scenarios, where the intensity of
309 selection on CT_{max} and/or *z* might be relatively weak. We acknowledge that our approach is
310 only a rough estimate of the problem and that several caveats could be raised. For instance,
311 although there is a high positive correlation across species for parameters CT_{max} and *z* ($r =$
312 0.92 ; [23]), the **G** matrix used to simulate the hypothetical scenarios could overestimate the
313 additive genetic covariance in an outbred *Drosophila* population due to higher linkage
314 disequilibria in the DGRP lines [29]. However, for the time being, we believe that the present
315 conclusions may be broadly applicable.

316
317 In summary, our findings suggest that the genetic correlation between CT_{max} and *z*
318 impose constraints on thermal tolerance strategies. The simulations performed here highlight
319 the importance of considering the multivariate nature of thermal tolerance traits and their
320 genetic correlations when predicting evolutionary responses to climate change. Ultimately,
321 this can be achieved by utilizing approaches that measure thermal tolerances considering both
322 the duration and intensity of heat stress and its potential for evolution. Adopting such

323 integrative approaches will enable more accurate predictions of how species might respond
324 to increasing temperatures in a rapidly changing planet.

325

326 **Data accessibility**

327 Data files and code supporting analyses, figures and tables of this study are publicly available
328 on GitHub (https://github.com/felixpleiva/Genetic_variation_TDT). When using the code from
329 this manuscript, please cite it as: Leiva FP, Santos M, Niklitschek EJ, Rezende EL, & Verberk
330 WCEP. (2024). Paper data and code for: Genetic variation of heat tolerance in a model
331 ectotherm: an approach using thermal death time curves. Zenodo. DOI will be available here.

332 **Authors' contributions**

333 Félix P. Leiva: conceptualization, data curation, formal analysis, funding acquisition,
334 investigation, methodology, project administration, resources, software, validation,
335 visualization, writing – original draft preparation, writing – review and editing; Mauro Santos:
336 conceptualization, formal analysis, methodology, software, writing – original draft preparation,
337 writing – review and editing; Edwin J. Niklitschek: formal analysis, software, validation, writing
338 – review and editing; Enrico L. Rezende: conceptualization, investigation, writing – review and
339 editing; Wilco C.E.P. Verberk: conceptualization, formal analysis, funding acquisition,
340 investigation, methodology, resources, supervision, writing – review and editing. All authors
341 gave final approval for publication.

342 **Funding**

343 This work was supported by the Alexander von Humboldt Foundation; the National Agency for
344 Research and Development (ANID, Chile) [grant number Becas Chile 2018-72190288,
345 PIA/BASAL FB0002]; Ministerio de Ciencia e Innovación (Spain) [grant number PID2021-
346 127107NB-I00]; Generalitat de Catalunya [grant number 2021 SGR 00526]; the Distinguished
347 Guest Scientists Fellowship Programme of the Hungarian Academy of Sciences
348 (<https://mta.hu>); FONDECYT (Chile) [grant number 1211113]; and The Netherlands
349 Organisation for Scientific Research (grant number VIDI 016.161.321).

350 **Acknowledgements**

351 We thank Cecilia Balboa for kindly assisting with video checking.

352 **References**

- 353 1. 2019 IPCC, 2018: Global Warming of 1.5°C. An IPCC Special Report on the impacts of
354 global warming of 1.5°C above pre-industrial levels and related global greenhouse gas
355 emission pathways, in the context of strengthening the global response to the threat of
356 climate change, sustainable development, and efforts to eradicate poverty. Cambridge,
357 UK and New York, NY, USA: Cambridge University Press.
- 358 2. Huey RB, Stevenson RD. 1979 Integrating thermal physiology and ecology of
359 ectotherms: a discussion of approaches. *American Zoologist* , 357–366.
- 360 3. Rezende EL, Bozinovic F. 2019 Thermal performance across levels of biological
361 organization. *Philosophical Transactions of the Royal Society B* **374**, 20180549.
- 362 4. Pinsky ML, Selden RL, Kitchel ZJ. 2019 Climate-driven shifts in marine species ranges:
363 scaling from organisms to communities. *Annual review of marine science* **12**, 153–179.

- 364 5. Urban MC. 2015 Accelerating extinction risk from climate change. *Science* **348**, 571–
365 573.
- 366 6. Rudman Seth M., Greenblum Sharon I., Rajpurohit Subhash, Betancourt Nicolas J.,
367 Hanna Jinjoo, Tilk Susanne, Yokoyama Tuya, Petrov Dmitri A., Schmidt Paul. 2022
368 Direct observation of adaptive tracking on ecological time scales in *Drosophila*. *Science*
369 **375**, eabj7484. (doi:10.1126/science.abj7484)
- 370 7. Hoffmann AA, Hercus MJ. 2000 Environmental stress as an evolutionary force.
371 *BioScience* **50**, 217–226.
- 372 8. Gunderson AR, Dillon ME, Stillman JH. 2017 Estimating the benefits of plasticity in
373 ectotherm heat tolerance under natural thermal variability. *Functional Ecology* **31**, 1529–
374 1539.
- 375 9. Huey RB, Kingsolver JG. 1993 Evolution of resistance to high temperature in
376 ectotherms. *American Naturalist* , S21–S46.
- 377 10. Rezende EL, Tejedo M, Santos M. 2011 Estimating the adaptive potential of critical
378 thermal limits: methodological problems and evolutionary implications. *Functional*
379 *Ecology* **25**, 111–121.
- 380 11. Santos M, Castañeda LE, Rezende EL. 2011 Making sense of heat tolerance estimates
381 in ectotherms: lessons from *Drosophila*. *Functional Ecology* **25**, 1169–1180.
- 382 12. Hoffmann AA, Chown SL, Clusella-Trullas S. 2013 Upper thermal limits in terrestrial
383 ectotherms: how constrained are they? *Functional Ecology* **27**, 934–949.
- 384 13. Araújo MB, Ferri-Yáñez F, Bozinovic F, Marquet PA, Valladares F, Chown SL. 2013
385 Heat freezes niche evolution. *Ecology Letters* **16**, 1206–1219.
386 (doi:https://doi.org/10.1111/ele.12155)
- 387 14. Sunday JM, Bates AE, Dulvy NK. 2011 Global analysis of thermal tolerance and latitude
388 in ectotherms. *Proceedings of the Royal Society of London B: Biological Sciences* **278**,
389 1823–1830. (doi:https://doi.org/10.1098/rspb.2010.1295)
- 390 15. Sunday JM et al. 2019 Thermal tolerance patterns across latitude and elevation.
391 *Philosophical Transactions of the Royal Society B: Biological Sciences* **374**.
392 (doi:10.1098/rstb.2019.0036)
- 393 16. Leiva FP, Boerrigter JG, Verberk WCEP. 2023 The role of cell size in shaping responses
394 to oxygen and temperature in fruit flies. *Functional Ecology* **37**, 1269–1279.
395 (doi:10.1111/1365-2435.14294)
- 396 17. Burton T, Einum S. 2020 The old and the large may suffer disproportionately during
397 episodes of high temperature: evidence from a keystone zooplankton species.
398 *Conservation Physiology* **8**, coaa038.
- 399 18. Castañeda LE, Rezende EL, Santos M. 2015 Heat tolerance in *Drosophila subobscura*
400 along a latitudinal gradient: contrasting patterns between plastic and genetic responses.
401 *Evolution* **69**, 2721–2734.
- 402 19. Leiva FP, Santos M, Rezende EL, Verberk WCEP. 2024 Intraspecific variation of heat
403 tolerance in a model ectotherm: The role of oxygen, cell size and body size. *Functional*
404 *Ecology* **38**, 439–448. (doi:10.1111/1365-2435.14485)

- 405 20. Truebano M, Fenner P, Tills O, Rundle SD, Rezende EL. 2018 Thermal strategies vary
406 with life history stage. *Journal of Experimental Biology* **221**, jeb171629.
- 407 21. Verberk WCEP, Hoefnagel KN, Peralta-Maraver I, Flourey M, Rezende EL. 2023 Long-
408 term forecast of thermal mortality with climate warming in riverine amphipods. *Global*
409 *Change Biology* **29**, 5033–5043. (doi:10.1111/gcb.16834)
- 410 22. Verspagen N, Leiva FP, Janssen I, Verberk WCEP. 2020 Effects of developmental
411 plasticity on heat tolerance may be mediated by changes in cell size in *Drosophila*
412 *melanogaster*. *Insect Science* **27**, 1244–1256. (doi:10.1111/1744-7917.12742)
- 413 23. Rezende EL, Castañeda LE, Santos M. 2014 Tolerance landscapes in thermal ecology.
414 *Functional Ecology* **28**, 799–809.
- 415 24. Leiva FP, Santos M, Rezende EL, Verberk WCEP. 2023 Intraspecific variation on heat
416 tolerance in a model ectotherm: the role of oxygen, cell size and body size. *Functional*
417 *Ecology* (doi:10.1111/1365-2435.14485)
- 418 25. Mackay TF et al. 2012 The *Drosophila melanogaster* genetic reference panel. *Nature*
419 **482**, 173–178.
- 420 26. 2007 STATISTICA (data analysis software system).
- 421 27. Wolter KM. 2007 *Introduction to Variance Estimation*. New York, NY: Springer New
422 York. (doi:10.1007/978-0-387-35099-8)
- 423 28. Sokal RR, Rohlf FJ. 1995 *Biometry*. New York.
- 424 29. Mackay TFC, Huang W. 2018 Charting the genotype–phenotype map: lessons from the
425 *Drosophila melanogaster* Genetic Reference Panel. *WIREs Developmental Biology* **7**,
426 e289. (doi:10.1002/wdev.289)
- 427 30. Knapp SJ, Bridges-Jr WC, Yang M-H. 1989 Nonparametric confidence interval
428 estimators for heritability and expected selection response. *Genetics* **121**, 891–898.
- 429 31. R Development Core Team. 2023 *R: A language and environment for statistical*
430 *computing*. R Foundation for Statistical Computing, Vienna, Austria.
- 431 32. Leiva FP, Santos M, Rezende EL, Verberk WCEP. 2021 Paper data and code of
432 manuscript: Intraspecific variation on heat tolerance in a model ectotherm: effects of
433 body mass, cell size, oxygen and sex. Zenodo.
434 (doi:https://doi.org/10.5281/zenodo.5120028)
- 435 33. Lande R. 1979 Quantitative genetic analysis of multivariate evolution, applied to brain:
436 body size allometry. *Evolution* **33**, 402–416.
- 437 34. Lande R, Arnold SJ. 1983 The measurement of selection on correlated characters.
438 *Evolution* **37**, 1210–1226.
- 439 35. Diamond SE. 2017 Evolutionary potential of upper thermal tolerance: biogeographic
440 patterns and expectations under climate change. *Annals of the New York Academy of*
441 *Sciences* **1389**, 5–19. (doi:10.1111/nyas.13223)
- 442 36. Logan ML, Cox CL. 2020 Genetic constraints, transcriptome plasticity, and the
443 evolutionary response to climate change. *Frontiers in Genetics* **11**, 538226.

- 444 37. Santos M, Castañeda LE, Rezende EL. 2012 Keeping pace with climate change: what is
445 wrong with the evolutionary potential of upper thermal limits? *Ecology and Evolution* **2**,
446 2866–2880. (doi:10.1002/ece3.385)
- 447 38. Fowler K, Whitlock MC. 1999 The distribution of phenotypic variance with inbreeding.
448 *Evolution* **53**, 1143–1156. (doi:10.2307/2640818)
- 449 39. Falconer DS, Mackay TFC. 1996 Introduction to quantitative genetics. 4th edn. Pearson
450 Education India.
- 451 40. Endler JA. 1986 Natural selection in the wild. Princeton University Press.
- 452 41. Kingsolver JG, Hoekstra HE, Hoekstra JM, Berrigan D, Vignieri SN, Hill CE, Hoang A,
453 Gibert P, Beerli P. 2001 The Strength of Phenotypic Selection in Natural Populations.
454 *The American Naturalist* **157**, 245–261. (doi:10.1086/319193)
- 455 42. Grant PR, Grant BR, Huey RB, Johnson MTJ, Knoll AH, Schmitt J. 2017 Evolution
456 caused by extreme events. *Phil. Trans. R. Soc. B* **372**, 20160146.
457 (doi:10.1098/rstb.2016.0146)
- 458 43. Rodríguez-Trelles F, Tarrío R, Santos M. 2013 Genome-wide evolutionary response to a
459 heat wave in *Drosophila*. *Biol. Lett.* **9**, 20130228. (doi:10.1098/rsbl.2013.0228)
- 460 44. MacMillan HA. 2019 Dissecting cause from consequence: a systematic approach to
461 thermal limits. *Journal of Experimental Biology* **222**, jeb191593.
- 462 45. Lecheta MC et al. 2020 Integrating GWAS and Transcriptomics to Identify the Molecular
463 Underpinnings of Thermal Stress Responses in *Drosophila melanogaster*. *Frontiers in*
464 *Genetics* **11**, 658. (doi:10.3389/fgene.2020.00658)
- 465 46. Rolandi C, Lighton JRB, de la Vega GJ, Schilman PE, Mensch J. 2018 Genetic variation
466 for tolerance to high temperatures in a population of *Drosophila melanogaster*. *Ecology*
467 *and Evolution* **8**, 10374–10383. (doi:10.1002/ece3.4409)
- 468 47. Kellermann V, Overgaard J, Hoffmann AA, Fløjgaard C, Svenning J-C, Loeschcke V.
469 2012 Upper thermal limits of *Drosophila* are linked to species distributions and strongly
470 constrained phylogenetically. *Proceedings of the National Academy of Sciences* **109**,
471 16228–16233.
- 472 48. Leiva FP, Calosi P, Verberk WCEP. 2019 Scaling of thermal tolerance with body mass
473 and genome size in ectotherms: A comparison between water-and air-breathers.
474 *Philosophical Transactions of the Royal Society B: Biological Sciences* **374**, 20190035.
475 (doi:10.1098/rstb.2019.0035)
- 476 49. Rezende EL, Bozinovic F, Szilágyi A, Santos M. 2020 Predicting temperature mortality
477 and selection in natural *Drosophila* populations. *Science* **369**, 1242–1245.
- 478 50. Jørgensen LB, Malte H, Overgaard J. 2019 How to assess *Drosophila* heat tolerance:
479 Unifying static and dynamic tolerance assays to predict heat distribution limits.
480 *Functional Ecology* **33**, 629–642. (doi:10.1111/1365-2435.132)
- 481 51. Jørgensen LB, Malte H, Ørsted M, Klahn NA, Overgaard J. 2021 A unifying model to
482 estimate thermal tolerance limits in ectotherms across static, dynamic and fluctuating
483 exposures to thermal stress. *Scientific reports* **11**, 1–14.

484 52. Huey RB, Kearney MR. 2020 Dynamics of death by heat. *Science* **369**, 1163–1163.
485 (doi:10.1126/science.abe0320)

486